JACS
JOURNAL OF THE AMERICAN CHEMICAL SOCIETY
pubs.acs.org/JACS
Article

Cobalt-Catalyzed Enantioselective Cross-Electrophile Couplings: Stereoselective Syntheses of 5−7-Membered Azacycles

Zhaoming Ma, Wenqiang Xu, Yun-Dong Wu, and Jianrong Steve Zhou*

Cite This: J. Am. Chem. Soc. 2023, 145, 16464−16473
Read Online
ACCESS | Metrics & More | Article Recommendations | Supporting Information

ABSTRACT: Cobalt complexes of chiral pyrox ligands catalyzed enantioselective reductive couplings of nonconjugated iododienes with aryl iodides or alkenyl bromides. The reaction enabled stereoselective syntheses of 5−7-membered azacycles carrying quaternary stereocenters. Mechanistically, cross-electrophile selectivity originated from selective coupling of alkylcobalt(I) complexes generated after cyclization with aryl iodides.

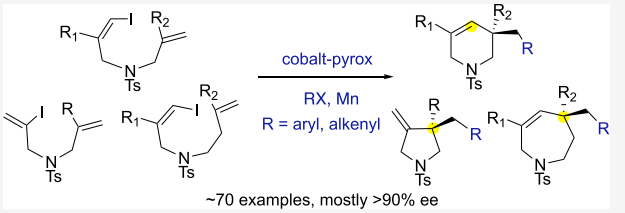

INTRODUCTION

Cobalt catalysts have been known to efficiently promote cross-electrophile couplings of two organic halides or other electrophiles in the presence of reductants,[1] but enantioselective variants of these reductive couplings are still very limited.[2] Recognizing this deficiency, we report herein a series of cobalt-catalyzed enantioselective cross-electrophile couplings of halodienes with aryl, heteroaryl, and alkenyl halides. The reactions enable stereoselective construction of partially saturated azacycles of 5−7 ring sizes, carrying new quaternary stereocenters (see Figure 1).[3] Pyrrolidines and piperidines are among the most frequently used rings in small-molecule drugs and drug candidates (for example, nifeviroc, paroxetine, and cisapride).[4] Azepine derivatives are also core structures in some medicines.[5] Mechanistically, a main challenge to form the desired azacycles is achieving the cross-electrophile selectivity.

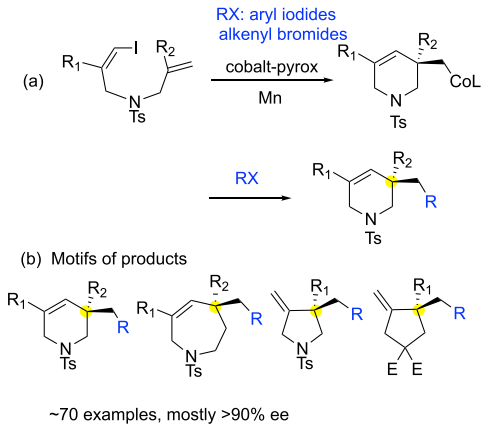

Figure 1. (a) Cobalt-catalyzed reductive couplings of iododienes with (hetero)aryl iodides and alkenyl electrophiles; (b) examples of 5−7-membered azacycles and carbocycles.

Recently, Shu et al.[6] reported nickel-catalyzed reductive couplings[7] of 1,6-halodienes and alkenyl electrophiles that stereoselectively formed pyrrolidines, oxacycles, and carbocycles, but the reaction was limited to the formation of five-membered rings. Typically, 5-exo-trig cyclization processes are faster than 6-exo-trig ones on transition metal complexes.

RESULTS AND DISCUSSION

Condition Optimization. Initially, we examined a model reaction of 1,6-iododiene **1a** and *o*-tolyl iodide in search for a suitable chiral cobalt catalyst in the presence of manganese powder (Figure 2).[8] After numerous attempts, we were gratified to identify that an in situ-formed precatalyst of $CoBr_2$(DME) and a 5-CF_3-pyrox **L1** provided desired piperidi-4-ene **2a** in good yields and 85% ees in dry THF. Without the cobalt catalyst, no conversion of the starting material was detected. We found that other 5-CF_3-pyrox **L2**-**L5** having *t*-Bu, *i*-Pr, *i*-Bu, *sec*-Bu, and Bn substituents afforded the product in slightly less than 90% ees. Moreover, when the reaction was conducted with pyrox **L4** at −10 °C, the product was formed in 89% yield and 93% ee. As a general trend, the cobalt catalysts of (*R*)-pyrox ligands gave (*R*)-isomer of **2a** as the major isomer. 5-CF_3-pyrox **L6** and **L7** having C4-phenyl rings on the oxazoline led to moderate ∼70% ees. In comparison, 5-F-pyrox **L8** and **L9** were slightly less stereoselective than the corresponding 5-CF_3-pyrox.

Pyrimidine-oxazolines **L10** and **L11** having *t*-Bu and *i*-Pr substituents led to 82−87% ees, whiles pyrazine-oxazoline **L12** was much less stereoselective (41% ee). Moreover, quinoline-

Received: March 18, 2023
Published: July 21, 2023

https://doi.org/10.1021/jacs.3c02829
J. Am. Chem. Soc. 2023, 145, 16464−16473

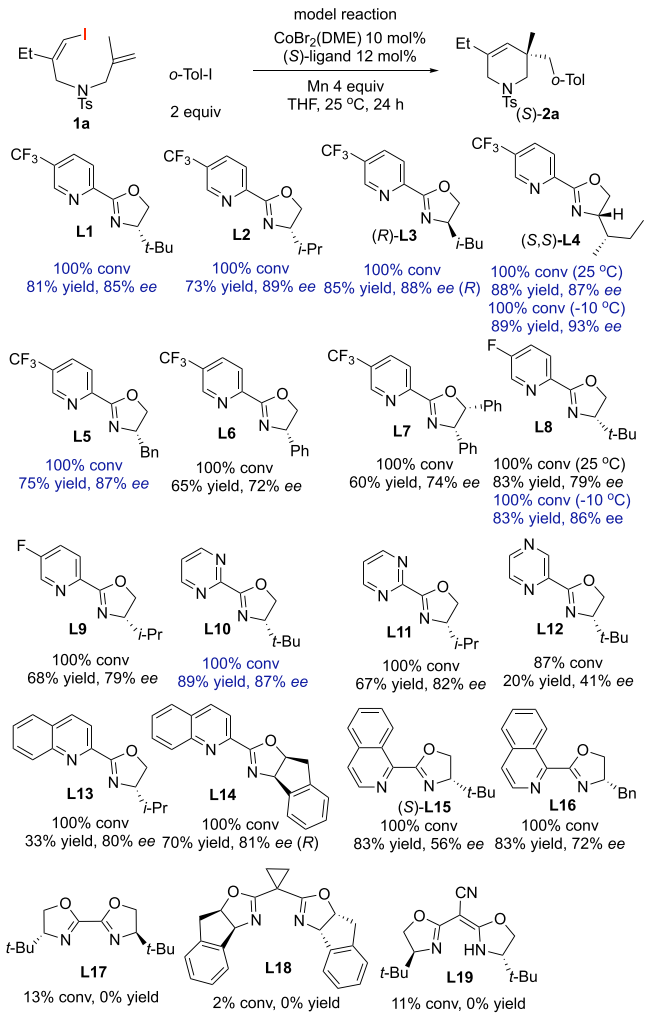

Figure 2. Optimization of chiral *N,N*-ligands for cobalt catalysts in asymmetric reductive coupling of **1a** and *o*-tolyl iodide (calibrated GC yields on 0.1 mmol scale in 0.3 mL of solvents). DME = 1,2-dimethoxyethane. (*S*)-**2a** was formed as the major isomer, unless it is specifically indicated as (*R*).

oxazoline **L13** and **L14** provided the product in around 80% ee, while isoquinoline-oxazolines **L15**–**L16** carrying *t*-butyl and benzyl substituents afforded moderate stereoselectivity. We also examined cobalt catalysts of bisoxazolines and semicorrins **L17**–**L19**, but they did not form active catalysts.

The choice of solvents proved to be critical in the reductive coupling of 1-iodo-1,6-diene **1a** and *o*-tolyl iodide (Table 1). For instance, in DMF, a full conversion of **1a** occurred at rt. after 24 h but giving **2a** in ∼30% yield and 70% ee (entry 3). The reaction in DMSO was very slow and gave only <30% conversion of **1a** (entry 4). In toluene and 1,1,1-trifluorotoluene (entries 5–6), ethereal solvents Et_2O, *n*-Pr_2O, and 1,4-dioxane (entries 7–9), the reaction proceeded very sluggishly to give <35% conversion, and no desired product was formed. However, in 1,2-dimethoxyethane (DME), THF, or 2-MeTHF (entries 10–14), we detected moderate-to-good yields of product **2a**. The result was improved to 76% yield and 92% ee by conducting the reaction at −10 °C in 2-MeTHF (see entry 14).

The use of 10 mol % of the cobalt catalyst led to a satisfactory formation of **2a** in 89% yield and 88% ee in 2-MeTHF at rt. (entry 15). The yield is significantly higher than

Table 1. Condition Optimization of Cobalt-Catalyzed Reductive Coupling of 1a and *o*-Tolyl Iodide (Calibrated GC Yields on 0.1 mmol Scale in 0.3 mL of Solvents)

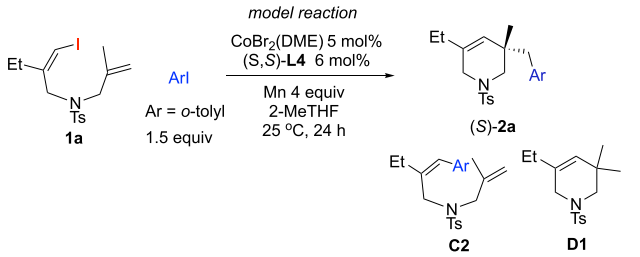

entry	conditions	conv (%)	2a (%)	ee (%)	C2 (%)	D1 (%)
1	no change	100	55	84	5	7
2	ArI 2 equiv	100	66	82	4	10
3	DMF as solvent	95	32	70		8
4	DMSO	26	9			23
5	toluene	35	0			
6	$PhCF_3$	31	0			
7	Et_2O	11	0			
8	*i*-Pr_2O	13	0			
9	1,4-dioxane	8	0			
10	DME	100	72	87	8	5
11	DME, −10 °C	87	41	90	2	5
12	THF	100	66	87	3	6
13	THF, −10 °C	100	63	90		5
14	2-MeTHF, −10 °C	100	76	92		5
15	[Co] 10 mol %	100	89	88		3
16	[Co] 2 mol %	100	49	84	6	9

a maximal theoretical yield of 71% where two halides in a ratio of 1:1.5 coupled statistically (without any selectivity of homo- vs heterocoupling).

The use of 2 mol % catalyst led to a slower conversion of **1a** and 49% yield of **2a** (entry 16). Additionally, the model reaction did not proceed at all without Mn powder. It gave a poor yield (<10%) of **2a** when zinc dust was employed instead.

Thus, under a typical condition consisting of 5 mol % cobalt, 6 mol % pyrox **L3** or **L4** in 2-MeTHF, **1a** (0.1 mmol) and aryl iodide (1.5 equiv) reacted to give product **2a** in 76% yield and 92% ee. The reactions completed at −10 °C after 24 h. Notably, the catalytic reaction formed a significant amount of biaryls under all the conditions.

In coupling with iododiene **1a**, *o*-tolyl bromide reacted very slowly and only gave 10% product of **2a** at 25 °C after 24 h. Phenyl chloride, triflate, and tosylate did not react due to difficulty in oxidative addition.

We also tested the tolerance of acidic groups and nitrogen-based functional groups in the model reaction of **1a** and *o*-tolyl iodide, using pyrox **L4**. 1 equiv. of water or phenol led to protonolysis of the key intermediate to form side product **D1**, while aniline, pyridine, or isoquinoline completely inhibited the cobalt catalysis. With 1 equiv of (−)-menthol, *t*-butanol, or phenyl acetylene, the model reaction still gave product **2a** in good yield, along with ∼20% of **D1**.

Substrate Scope. With the optimized conditions in hand, we examined the scope of (hetero)aryl iodides in reactions with 1-iodo-1,6-diene **1a** using a cobalt catalyst of 5-CF_3-pyrox (*R*)-**L3** (Figure 3A). A wide range of aryl iodides reacted smoothly to give desired products in good yields and excellent ees in 2-MeTHF at −10 °C. The aryl halides can have *i*-Pr and

https://doi.org/10.1021/jacs.3c02829
J. Am. Chem. Soc. 2023, 145, 16464−16473

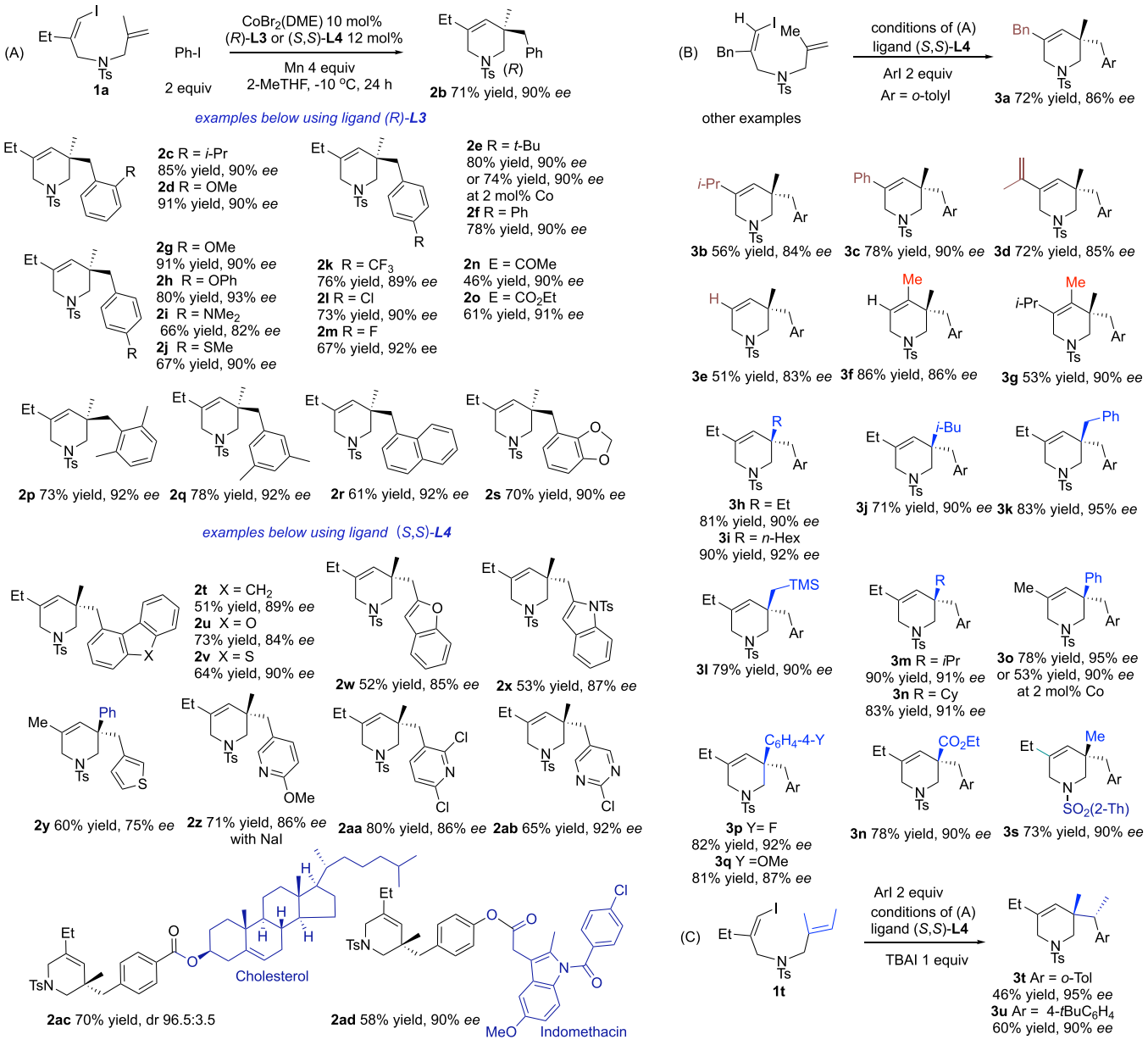

Figure 3. Substrate scope of (A) aryl and heteroaryl iodides and (B) iododienes and (C) **1t** in asymmetric reductive couplings to form piperidi-4-enes (isolated yields on 0.1 mmol scale in 0.3 mL of solvent).

OMe groups at *ortho* positions (**2c−d**) as well as electron-withdrawing phenyl, CF_3, chlorine, fluorine, ketone, and ester (**2e−j**), and electron-donating *t*-Bu, OMe, OPh, NMe_2, and SMe groups at *para* positions (**2k−o**).

Other aryl iodides included those derivatives of 2,6-xylyl and 3,5-xylyl (**2p−q**), 1-naphthyl (**2r**), 1,3-benzodioxole (**2s**), fluorene, dibenzofuran, and dibenzothiophene (**2t−v**). A single crystal of compound **2v** was obtained from vapor diffusion of pentane to aa solution in dichloromethane. X-ray diffraction analysis established its absolute configuration to be 3*S*. Additionally, many types of heteroaryl iodides coupled efficiently, including those of benzofuran (**2w**), indole (**2x**), thiophene (**2y**), 2-methoxypyridine (**2z**), 2,6-dichloropyridine (**2aa**), and 2-chloropyridmidine (**2ab**). Unfortunately, 3-pyridyl iodide led to a low yield probably due to inhibitory binding of pyridine to the cobalt catalyst. Furthermore, aryl iodides also coupled efficiently when they are attached to structurally complex cholesterol and indomethacin (**2ac−ad**).

Next, we explored the scope of iododienes in stereoeselective couplings with *o*-iodotoluene that formed substituted piperidienes. Commercially available (*S*,*S*)-**L4** gave products with similarly high ees as (*R*)-**L3**, so **L4** was used in our subsequent studies (Figure 3B). We found that various groups can be present at C3-positions of piperidi-3-enes, such as methyl ethyl, benzyl (**3a**), isopropyl (**3b**), phenyl (**3c**), isopropenyl (**3d**), and even a hydrogen (**3m**). Moreover, a methyl at the C4 positions did not inhibit the desired 6-exo-trig cyclization (**3f−g**). Many substituents were also well tolerated at C5 positions of piperidienes such as ethyl, *n*-hexyl and isobutyl (**3h−j**), benzyl and trimethylsilylmethyl (**3k−l**), isopropyl and cyclohexyl (**3m−n**), aryl rings (**3o−q**), and an ester (**3n**). Moreover, the *N*-tosylamide linker in the iododienes can be replaced by a 2-thienylsulfonylamide.

Notably, reductive coupling of iododiene **1t** with aryl halides gave products **3t** and **3u** in 46% and 60% yields and both in >90% ees (Figure 3C). Both products contain a quaternary

https://doi.org/10.1021/jacs.3c02829
J. Am. Chem. Soc. 2023, 145, 16464−16473

stereocenter and a tertiary stereocenter on vicinal carbons. *n*-Bu_4NI was added to improve yields.

We also examined some catalytic reactions using 2 mol % cobalt catalyst of **L4** to determine its catalytic efficiency (at −10 °C for 60 h). The conditions gave slightly lower yields of products (e.g., **2e** in 74% yield and **3 h** in 61% yield), mainly owing to incomplete conversion.

As shown in Figure 4, stereoselective reductive couplings of iododienes also coupled well with alkenyl bromides as coupling

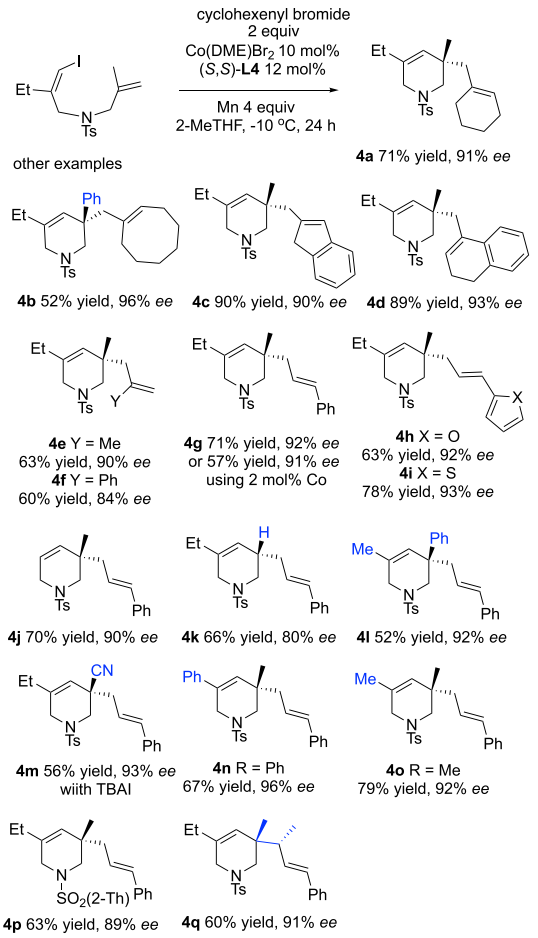

Figure 4. Asymmetric reductive couplings of iododienes with various alkenyl bromides to form piperidi-4-enes (isolated yields from reactions at 0.1 mmol scale in 0.3 mL of solvent).

partners. Thus, various alkenyl groups can be installed on piperidienes, such as 1-cyclohexenyl (**4a**), 1-cyclooctenyl (**4b**), 2-indenyl (**4c**), 3,4-dihydro-1-napthalenyl (**4d**), isopropenyl (**4e**), *α*-styrenyl (**4f**), (*E*)-*β*-styrenyl (**4g**), (*E*)-*β*-(2-furyl)-ethenyl (**4 h**), and (*E*)-*β*-(2-thienyl)ethenyl groups (**4i**). Notably, (*E*)-*β*-styrenyl iodide homocoupled to form a significant amount of a 1,3-diene when it was subjected to a domino coupling with **1a**.

The domino couplings also tolerated well structural variations in 1-iodo-1,6-dienes, for example, methyl (**4l**), ethyl (**4k**), a hydrogen atom (**4j**), and phenyl (**4n**) groups can be present on the C3 positions in products. On the C5-positions of piperidi-4-enes, methyl (**4j**), phenyl (**4l**), and hydrogen (**4k**) can be installed. Again, the *N*-tosylamide linker in substrates can be switched to 2-thienylsulfonylamide (**4p**). Additionally, a challenging coupling of iododiene **1t** was achieved with (*E*)-*β*-bromostyrene to afford product **4q** in 63% yield and 89% ee, which contains two contiguous stereocenters, one quaternary and another tertiary. Unfortunately, alkenyl triflates and acetates did not react with **1a** to give the coupling products.

Catalytic methods for enantioselective syntheses of monocyclic azepine and its derivatives are still limited today.[9] 7-Exo-trig cyclization on transition metal complexes is slower than those forming 5- and 6-membered rings. It is also challenging to achieve high levels of enantiofacial cyclization to form seven-membered ring formation due to conformational flexibility.[10]

Gratifyingly, we discovered that the cobalt catalyst of pyrox **L4** efficiently promoted asymmetric reductive coupling of (*Z*)-1-iodo-1,7-diene **5a** with various aryl iodides in excellent stereocontrol (see Figure 5). For example, **5a** reacted with *o*-

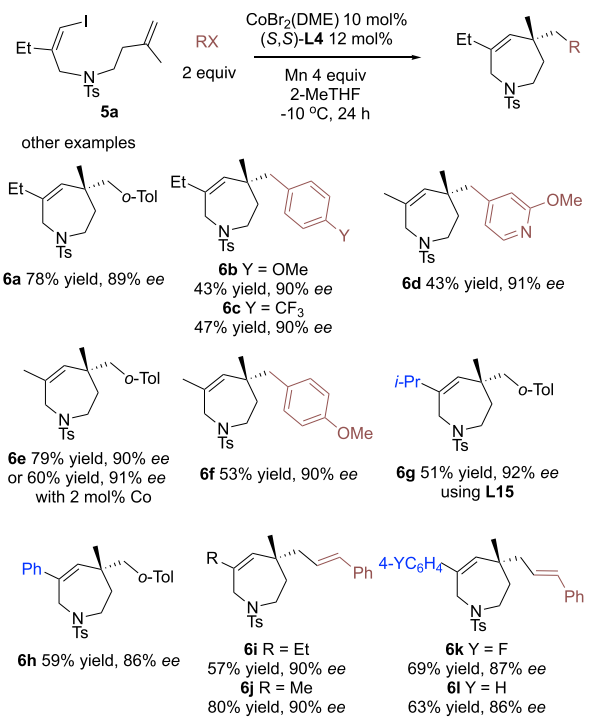

Figure 5. Stereoselective formation of azepine derivatives via asymmetric reductive couplings using pyrox **L4** (isolated yields on 0.05 mmol scale in 0.3 mL of solvent).

tolyl iodide to afford product **6a** in 78% yield and 89% ee. In some cases that gave moderate yields of products **6b−d**, premature reductive coupling with aryl iodides led to noncyclized side products **C2** (see the catalytic cycle below). The catalytic in reductive coupling also proceeded well with alkenyl halides (**6i−l**). For example, the reaction of **5a** with (*E*)-styrenyl bromide provided **6j** in 80% yield and 90% ee.

Structural variations on 1-iodo-1,7-dienes were also tolerated, for example, the C2 positions in the products can have methyl (**6e**), isopropyl (**6g**), phenyl (**6h**), and other aryl rings (**6k**). In the cyclization to form **6g**, the yield was only 37%. It was improved 51% yield after we switched the ancillary ligand from pyrox **L4** to isoquinox **L15**, while at the same time providing identical 92% ee.

We have successfully applied the cobalt catalyst of isoquinox **L15** to stereoselective syntheses of pyrrolidines having new quaternary stereocenters on C3 positions (Figure 6). Thus, the reaction of 2-iodo-1,6-diene **7a** with (*E*)-styrenyl bromide

https://doi.org/10.1021/jacs.3c02829
J. Am. Chem. Soc. 2023, 145, 16464−16473

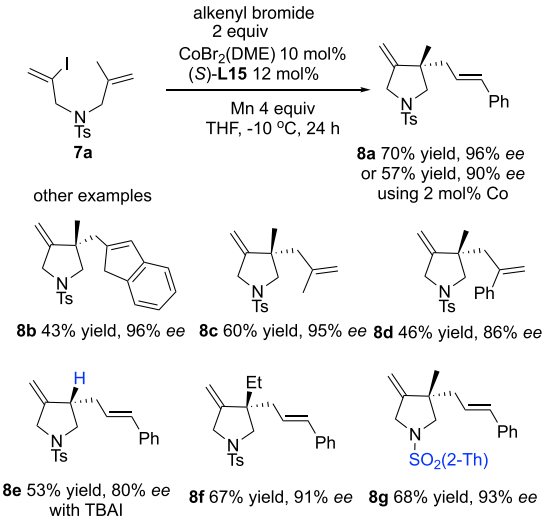

Figure 6. Substrate scope of iododienes and alkenyl halides in asymmetric reductive couplings using pyrox **L1** that formed pyrroldines (isolated yields on 0.1 mmol scale in 0.3 mL of solvent).

afforded product **8a** in 70% yield and 96% ee. In comparison, the cobalt catalyst of pyrox **L4** only provided the product in ~80% ee. Other alkenyl bromides underwent reductive couplings smoothly (**8b**−**8d**). Notably, a new tertiary stereocenter was forged in product **8e** in 89% ee. In this reaction, adding 1 equiv of *n*-Bu_4NI improved its yield from 36 to 53%. This method was also employed to prepare pyrrolidine **8 g** carrying an *N*-(2-thienyl)sulfonylamide.

The iododienes were not limited to those having *N*-sulfonamides as linkers. For example, 2-iodo-2,6-diene **7h** having a malonyl linker also smoothly reacted with simple alkenyl halides to afford cyclopentanes **8h**−**8i** in 84−94% ees (eq 1).

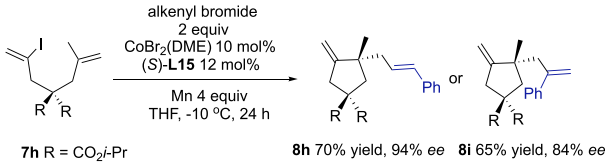

Product Derivatization. We then conducted some derivatization reactions of domino coupling products (Figure 7). For example, the allylic amide fragment was isomerized to give enamide **9a** (65% yield after 70% conv) by heating with a stoichiometric amount of $Co_2(CO)_8$. SeO_2 oxidation led to the formation of dihydropyridin-4-one **9b** in 61% yield. Additionally, fluorination using Selectfluor occurred in a regio- and

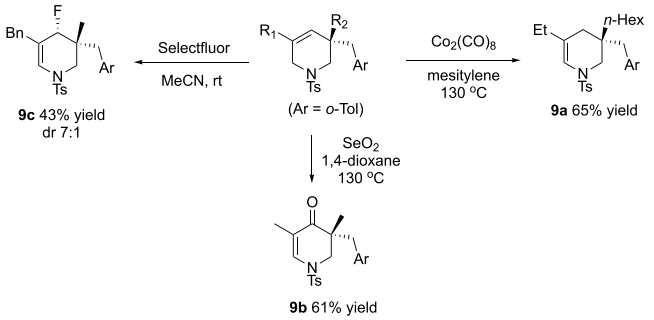

Figure 7. Product derivatization.

stereoselective fashion to give allylic fluoride **9c** (43% yield and 7:1 dr). The fluorine was added *trans* to the axial methyl group in a half-chair conformation, based on an NOE analysis.

MECHANISTIC STUDIES

Catalytic Cycle. Previously, Gosmini et al. proposed oxidative addition of aryl and alkenyl halides on cobalt[I]

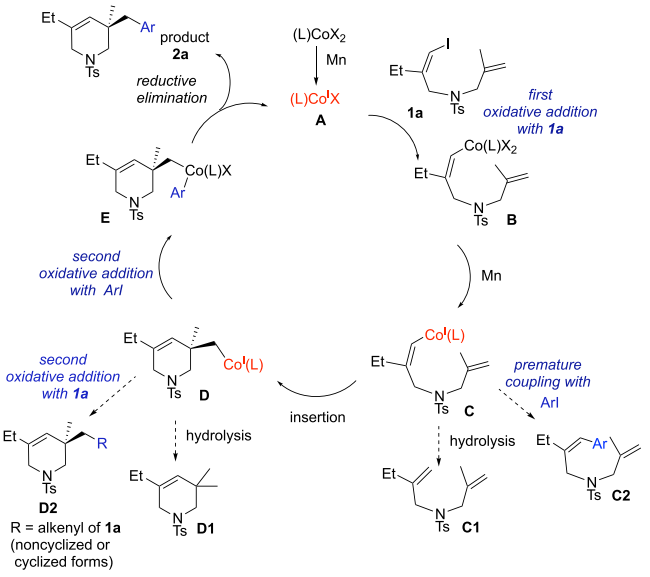

Figure 8. Putative catalytic cycle.

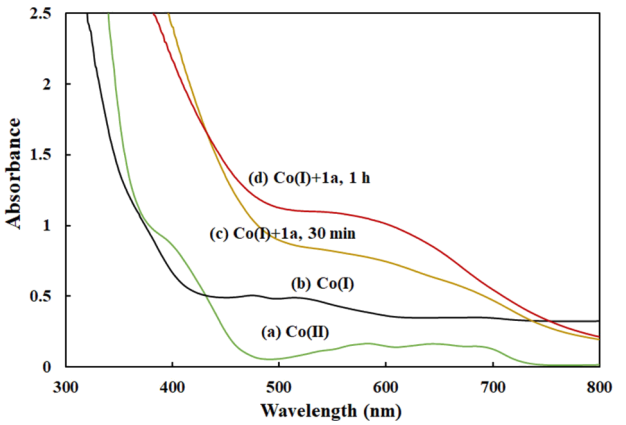

Figure 9. UV-ultra red spectra. (a) (**L4**)$Co^{II}Br_2$ was prepared from $CoBr_2$(DME) (0.03 mmol) and (*S*,*S*)-**L4** (0.03 mmol) and dry THF (0.6 mL). (b) Reduction with Mn powder (0.30 mmol, 10 equiv) produced (**L4**)$Co^{I}Br$ for 30 min. (c) Iododiene **1a** (1.7 equiv to Co) was then reacted with (**L4**)$Co^{I}Br$ for 30 min and (d) for 1 h. Each time, 0.1 mL of the solution was taken, filtered through an Acrodisc, and diluted with 3 mL of THF in a dry cuvette for the UV-ultra red measurement.

complexes and C−C reductive elimination on cobalt[III] based on DFT calculations.[11] We thus propose a catalytic cycle for our cobalt-catalyzed reductive coupling (Figure 8). Oxidative addition of in-situ-formed cobalt[I] **A** with iododiene **1a** produces alkenyl cobalt[III] **B**. The latter is reduced by Mn to give alkenyl cobalt[I] **C** which readily undergoes 6-exo-trig cyclization to form alkyl cobalt[I] **D**. Oxidative addition of complex **D** with aryl iodide later generates alkyl aryl cobalt[III] species **E** which eventually undergoes C−C reductive

https://doi.org/10.1021/jacs.3c02829
J. Am. Chem. Soc. 2023, 145, 16464−16473

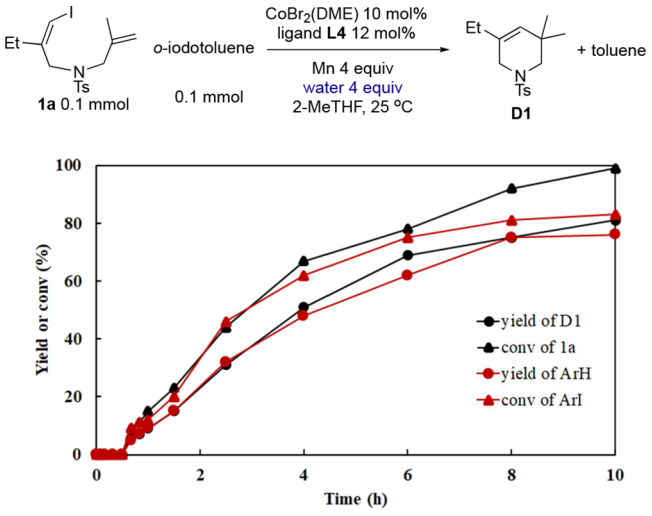

Figure 10. Kinetics of the reaction of iododiene **1a** and *o*-tolyl iodide in the *presence* of water (GC conversions of **1a** and *o*-tolyl iodide and calibrated yields of toluene and **D1**). Conditions: **1a** (0.1 mmol), *o*-tolyl iodide (0.1 mmol), Co(*DME*)Br_2 (0.01 mmol), **L4** (0.012 mmol), Mn powder (0.4 mmol), GC standard *n*-$C_{16}H_{34}$ (10 μL) sand water (0.4 mmol) in dry 2-MeTHF (0.6 mL). The reaction was stirred at rt. and aliquots were taken at intervals for GC analysis to determine conversions of **1a** and *o*-tolyl iodide and calibrated yields of products **D1** and toluene.

elimination to give final product **2a**.[12] Complexes of cobalt^{I} **C** and **D** can react with water or alcohols if they are present in the reaction.

To gain mechanistic insights into the oxidative addition of cobalt, we carried out Mn reduction of in-situ-formed complex (**L4**)$Co^{II}Br_2$ in THF and monitored with UV-ultra red spectroscopy (Figure 9). (a) A green solution (**L4**)$Co^{II}Br_2$ showed three distinct absorption signals in the range of 580–700 nm, which correspond to d-d transitions of high-spin tetrahedral complexes of cobalt^{II}.[13] (b) Its reduction with 10 equiv of Mn powder gave a black solution of (**L4**)Co^{I}Br **A** with two weak absorbance peaks around 500 nm.[13d] (c, d) Subsequent treatment of this solution of complex **A** with 1.7 equiv of iododiene **1a** slowly afforded a broad signal at 500–700 nm over 1 h. No signals of cobalt^{II} complexes were visible. At the end of the reaction, the mixture was passed through a silica gel plug and subjected to GC analysis. Most of **1a** was converted to hydrolytic product **D1** in 68 and 78% yields after 30 min and 1 h, respectively (eq 2). The formation of side product **D2** was negligible.

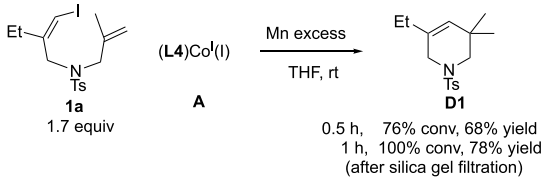

When the stoichiometric reaction of **1a** and (**L4**)Co^{I}(I) was conducted in DMF, *m*/*z* signals of $[M + H]^+$ corresponding to putative complexes **A** and **D** were detected by ESI-HRMS (see the Supporting Information).

Cross-Electrophile Selectivity. To probe the origin of cross-electrophile selectivity, we added 4 equiv of water to the model reaction of iododiene **1a** and *o*-tolyl iodide and gained some insights into the activation of these electrophiles (see Figure 10). (a) The putative complexes alkyl cobalt **D** and

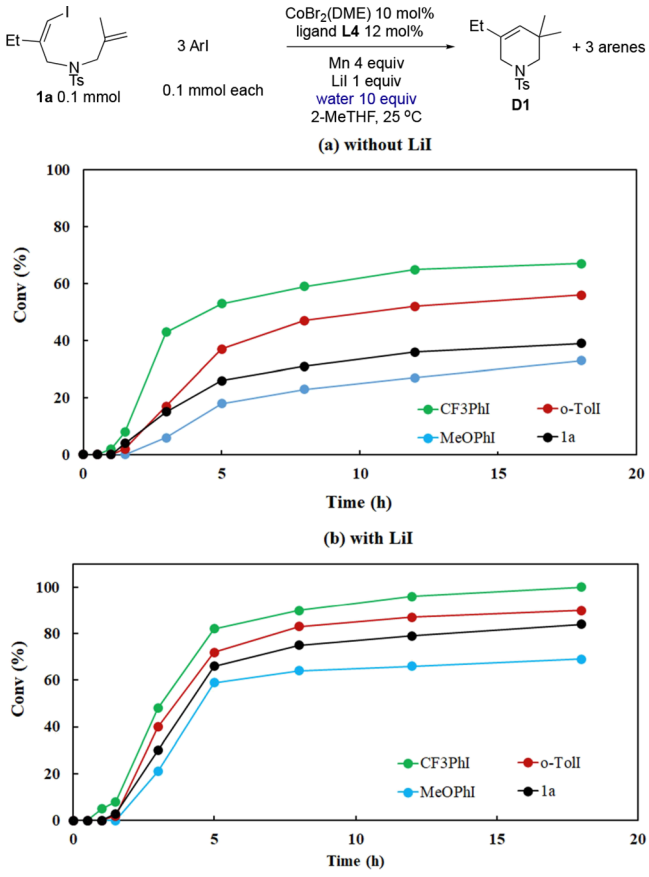

Figure 11. Kinetics of a competition reaction of iododiene **1a** with *p*-CF_3PhI, *o*-tolyl iodide, and *p*-MeOPhI in the *presence* of water: (a) GC conversion of aryl iodides and **1a** without LiI and (b) with LiI. Conditions: **1a** (0.1 mmol), aryl iodides (0.1 mmol each), Co(DME)Br_2 (0.01 mmol, 10 mol %), (*S*,*S*)-**L4** (0.012 mmol), Mn powder (0.4 mmol), LiI (0.1 mmol), and water (1.0 mmol, 10 equiv) in dry 2-MeTHF (0.6 mL).

analogous aryl cobalt species were quickly hydrolyzed by water to form piperidiene **D1** and toluene, both in >80% yields, respectively. (b) Neither a homocoupling of **1a** nor heterocoupling of two organic halides was detected. Thus, Mn reduction of alkenyl cobalt^{III} **B** and cyclization of alkenyl cobalt(I) **C** to form alkyl cobalt species **D** are faster than hydrolysis by water. (c) We detected an induction period of about 0.5 h for Mn reduction of (*L*)CoX_2 to form active catalyst (*L*)CoX **A**.

In the model coupling of **1a** and *o*-iodotoluene, side product **D2** was formed in a very small amount (<5%). It was derived from coupling of complex **D** with a second molecule of **1a** (in the cyclized or noncyclized form of the dienyl fragment). Thus, the first oxidative addition of catalyst **A** can occur with both **1a** and aryl iodides, but alkyl cobalt^{I} **D** showed a high preference for oxidative addition of aryl iodides to produce **2a**. The biaryl was also formed as the main side product via a nonproductive path of oxidative addition of ArX, Mn reduction, and a second oxidative addition of ArX.

Next, we subjected iododiene **1a** to a competition with three aryl iodides in one vessel, including *p*-CF_3PhI, *o*-tolyl iodide, and *p*-MeOPhI (see Figure 11). After an induction period for activation of the cobalt precatalyst, initial rates of aryl iodides and **1a** were found to follow the following order—*p*-CF_3PhI > *o*-tolyl iodide > iododiene **1a** > *p*-MeOPhI. The trend

https://doi.org/10.1021/jacs.3c02829
J. Am. Chem. Soc. 2023, 145, 16464–16473

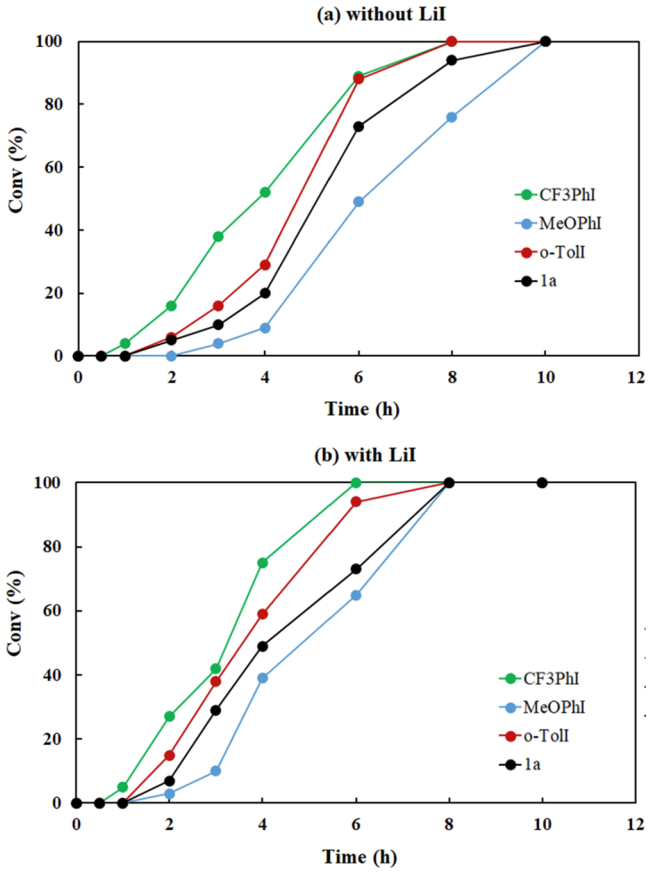

Figure 12. Kinetics of competition reactions of iododiene **1a** with *p*-CF_3PhI, *o*-tolyl iodide, and *p*-MeOPhI in one vessel, in the *absence* of water under similar conditions described in Figure 11. (a) GC conversion of aryl iodides and **1a** without LiI and (b) with LiI.

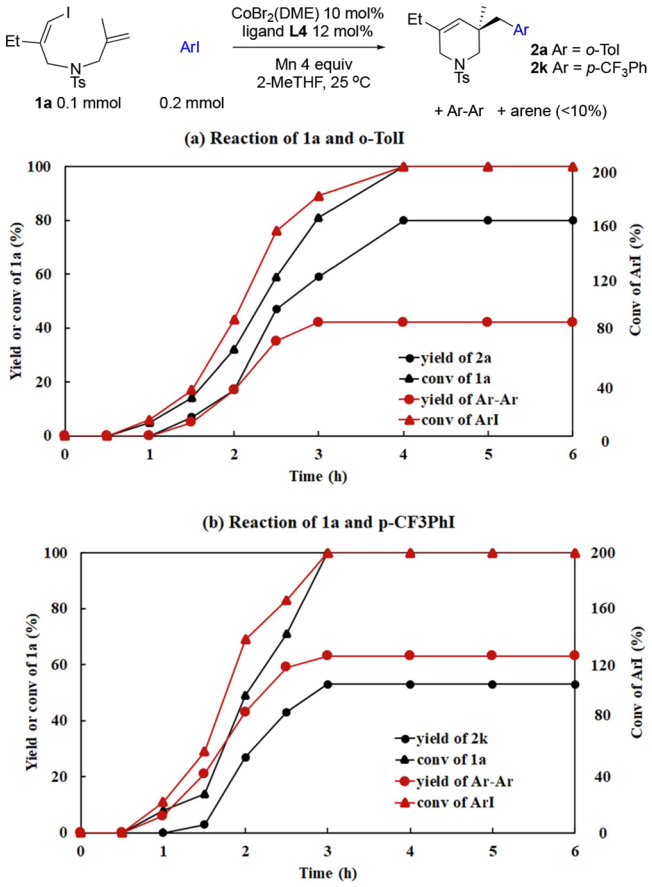

Figure 13. Kinetics of individual catalytic couplings of iododiene **1a** with (a) *o*-tolyl iodide and (b) *p*-CF_3PhI in the *absence* of added water. Conditions: **1a** (0.1 mmol), aryl iodide (0.2 mmol, 200 mol %), Co(*DME*)Br_2 (0.01 mmol, 10 mol %), (*S,S*)-**L4** (0.012 mmol), Mn powder (0.4 mmol) in dry 2-MeTHF (0.6 mL).

suggested that the first oxidative addition followed a common electronic effect of aryl iodides. When 1 equiv of LiI was added, initial rates of aryl iodides and **1a** were significantly increased, and at the same time, the rate difference of the organic halides became smaller. This suggested that Mn reduction contributed to the rate-limiting steps in the first half catalytic cycle (**A** → **D**). Ethyl *p*-bromobenzoate was unreactive in a competition with **1a**.

We also conducted competition experiments in one vessel *without* added water to study the relative reactivity of organic halides in entire catalytic cycles (Figure 12). The trend of reaction rates of three aryl halides and iododiene **1a** remained the same—*p*-CF_3PhI > *o*-tolyl iodide > iododiene **1a** > *p*-MeOPhI (52, 29, 20 and 9% conversions at 4 h). Addition of 1 equiv of LiI significantly increased the rate of consumptions of the organic halides (75, 59, 49, and 39% conversions at 4 h, respectively). Thus, we conclude that oxidative addition of organic halides contributed to the overall rates. LiI can speed up the entire catalytic cycle by accelerating the steps involving Mn reduction.

When individual catalytic reactions of **1a** and aryl iodides were conducted in *separate* vessels (see Figure 13), both reactions were completed within 4 h in the presence of 10 mol % cobalt catalyst, providing products **2a** (80%) and **2k** (53%). Concomitantly, biaryls were formed as main side products (final yields of 42 and 63%, respectively). The formation of arenes from ArX was minimal (<10%). Notably, the consumption of *o*-tolyl iodide was slower than *p*-CF_3PhI (45% versus 69% conversion after 2 h), confirming that oxidative additions contributed to the overall rates of the catalytic reactions. Notably, the catalytic reaction of *p*-CF_3PhI produced a significant amount of isomers **D2** at rt. The formation of **D2** isomers was temperature-sensitive and it was minimized when the catalytic reaction was conducted at −10 °C (forming 76% yield of **2k**, see Figure 3).

Halide Effect. We have conducted kinetic studies on the model coupling reaction of **1a** and *o*-tolyl iodide using 2 mol % $CoBr_2$(DME) and **L4** by adding 1 equiv of LiI, NaI, NaBr, or TBAI (see Figure 14a). Without the halides, there was a long induction period of 8 h. LiI, NaI, and NaBr not only greatly shortened the induction period to 2 h but also accelerated the overall rates of the model catalytic reactions (reaching half conversion of **1a** after 3−5 h). The formation of side product **D1** mostly accounted for material balance of **1a** in the reactions (Figure 14b). Thus, we believe that the halides accelerated Mn reduction of the cobalt precatalyst and intermediates in the catalytic cycle by facilitating dissociation of the reduced complexes from active sites of manganese surface via halide exchange.[14] TBAI also shortened the induction period, but its effect on the overall reaction rate was more moderate (reaching a half conversion after 14 h). Notably, TBAI improved the final yield of product **2a** from ~60 to 80% after 24 h. The model reaction of **1a** with 1 equiv

https://doi.org/10.1021/jacs.3c02829
J. Am. Chem. Soc. 2023, 145, 16464−16473

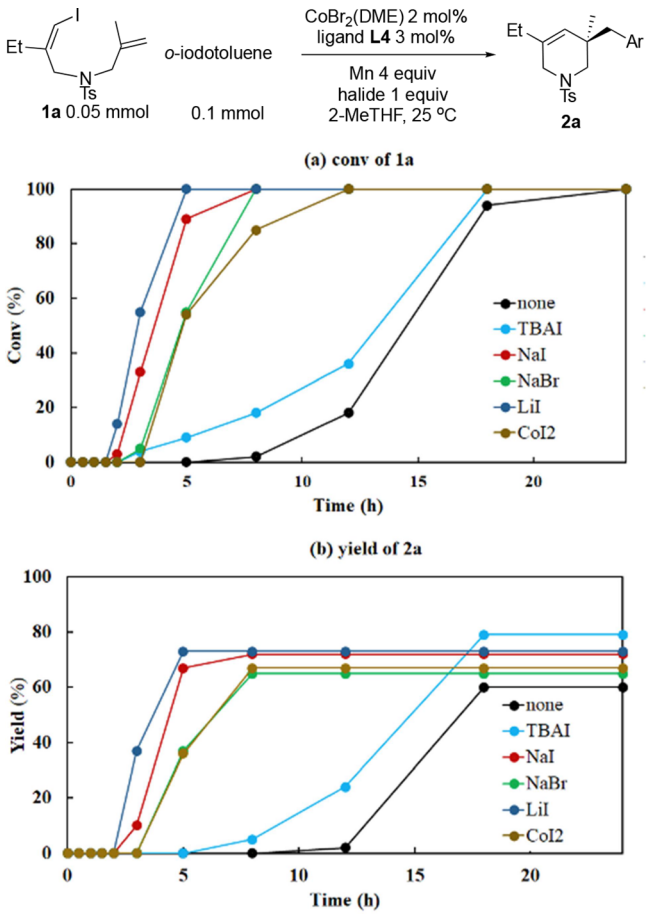

Figure 14. Kinetic studies of halide additives on the model catalytic reaction of iododiene **1a** and *o*-tolyl iodide in the presence of 2 mol % cobalt catalyst of **L4**: (a) GC conversion of **1a** and (b) calibrated GC yield of **2a**. Conditions: **1a** (0.05 mmol), *o*-tolyl iodide (0.1 mmol), Co(*DME*)Br_2 (1 μmol, 2 mol %), **L4** (1.5 μmol, 3 mol %), Mn powder (0.2 mmol) and halide salt (0.05 mmol) in dry 2-MeTHF (0.6 mL). Co(*DME*)Br_2 was replaced by CoI_2 (1 μmol). The reaction was stirred at rt. and aliquots were taken at intervals for GC analysis to determine the conversions of **1a** and calibrated yields of product **2a**.

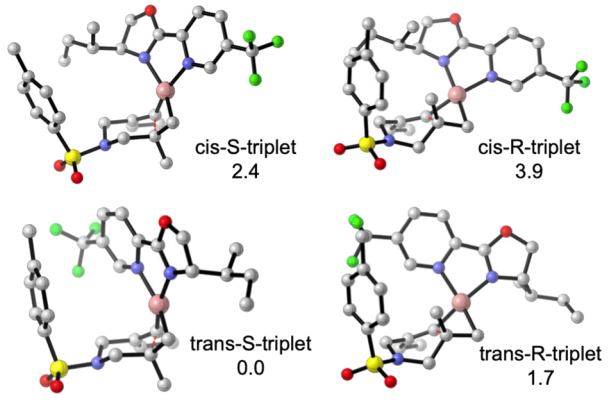

Figure 15. Four triplet transition states of cyclization of alkenyl cobalt^{I} complex **C** and relative values of Gibbs free energies in kcal mol^{-1}. In the ball-and-stick representations, the migrating alkenyl group on cobalt is shown at the back and the isobutene moiety in the front.

of TBAOTf became slightly faster, but it was still much slower than that with TBAI.

We also conducted a model reaction using a catalytic amount of CoI_2. The induction period was shortened and the catalytic reaction became faster and the final yield of **2a** was 67%.

Equipped with the knowledge of the halide effect, we scaled up the model reaction of **1a** to 0.3 mmol and obtained product **2a** in 71% yield and 89% ee using 5 mol % cobalt and 1 equiv of TBAI at 0 °C (eq 3). At 2 mol % cobalt, the reaction gave 52% yield of **2a** and more side product **C2**.

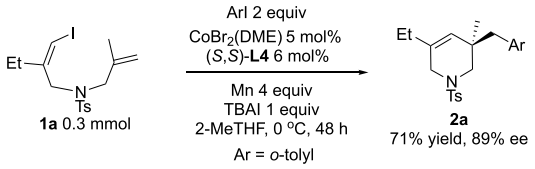

DFT Calculation. We also conducted DFT calculations to examine the insertion step of alkenyl cobalt^{I} complex **C**. The calculations were performed using SMD(2-MeTHF),B3LYP-D3/6-311+G(d,p); SDD(Co)//B3LYP-D3/6-31g(d); LANL2DZ(Co) level of theory. We made a few conclusions. (a) Gibbs free energies of triplet transition states (TS) for the insertion are much lower than those of singlet TSs by 11−14 kcalmol^{-1}, respectively. (b) Among the four triplet TSs (see Figure 15), two *trans* structures position the migrating alkenyl group *trans* to the oxazoline of **L4** which is more donating than pyridine. The free energies of two *trans* transition structures are lower than two *cis* structures, by about 2 kcal mol^{-1}. (c) Among them, chairlike structure *trans-S-triplet* has the lowest energy (with an insertion barrier of 15.9 kcal mol^{-1}), while TS *trans-R-triplet* is destabilized by its twist-boat-like conformation. (d) Free energies of TS *trans-S-3* and *trans-R-3* are 1.7 kcal mol^{-1} apart, which agrees well with 90% ee observed in the model reaction of **1a** that gave product **2a**.

CONCLUSIONS

In summary, we report a series of cobalt-catalyzed enantioselective reductive coupling reactions that produced 5−7-membered azacycles in excellent ees. Mechanistic studies revealed that the selective coupling of two different organic halides originated from the second oxidative addition in the catalytic cycle. Alkyl cobalt(I) species **D** showed a great preference to react with aryl iodides to form desired products rather than homocoupling with another molecule of iododienes to form side products **D2**.[15] The nonproductive formation of **D2** was temperature-sensitive and it may be impeded by a difficult *alkyl*−*alkyl* reductive elimination after 6-exo-trig cyclization of the second dienyl fragment on cobalt.

ASSOCIATED CONTENT

Supporting Information

The Supporting Information is available free of charge at https://pubs.acs.org/doi/10.1021/jacs.3c02829.

Experimental procedures and compound characterizations (PDF)

NMR spectra (PDF)

DFT calculations (PDF)

Accession Codes

CCDC 2204303 contains the supplementary crystallographic data for this paper. These data can be obtained free of charge via www.ccdc.cam.ac.uk/data_request/cif, or by emailing data_request@ccdc.cam.ac.uk, or by contacting The Cam-

https://doi.org/10.1021/jacs.3c02829
J. Am. Chem. Soc. 2023, 145, 16464−16473

bridge Crystallographic Data Centre, 12 Union Road, Cambridge CB2 1EZ, UK; fax: +44 1223 336033.

AUTHOR INFORMATION

Corresponding Author

Jianrong Steve Zhou − *State Key Laboratory of Chemical Oncogenomics, Guangdong Provincial Key Laboratory of Chemical Genomics, School of Chemical Biology and Biotechnology, Peking University Shenzhen Graduate School, Shenzhen 518055, China;* orcid.org/0000-0002-1806-7436; Email: jrzhou@pku.edu.cn

Authors

Zhaoming Ma − *State Key Laboratory of Chemical Oncogenomics, Guangdong Provincial Key Laboratory of Chemical Genomics, School of Chemical Biology and Biotechnology, Peking University Shenzhen Graduate School, Shenzhen 518055, China*

Wenqiang Xu − *Laboratory of Computational Chemistry and Drug Design, State Key Laboratory of Chemical Oncogenomics, Peking University Shenzhen Graduate School, Shenzhen 518055, China*

Yun-Dong Wu − *Laboratory of Computational Chemistry and Drug Design, State Key Laboratory of Chemical Oncogenomics, Peking University Shenzhen Graduate School, Shenzhen 518055, China;* orcid.org/0000-0003-4477-7332

Complete contact information is available at: https://pubs.acs.org/10.1021/jacs.3c02829

Notes

The authors declare no competing financial interest.

ACKNOWLEDGMENTS

We acknowledge financial support from the National Natural Science Foundation of China (NSFC 22271007), Peking University Shenzhen Graduate School, State Key Laboratory of Chemical Oncogenomics, Guangdong Provincial Key Laboratory of Chemical Genomics, Shenzhen Bay Laboratory and Shanghai Key Laboratory for Molecular Engineering of Chiral Drugs for J.S.Z. and National Natural Science Foundation of China (NSFC 21933004) for Y.D.W.

REFERENCES

(1) (a) Gosmini, C.; Bégouin, J.-M.; Moncomble, A. Cobalt-catalyzed cross-coupling reactions. *Chem. Commun.* **2008**, 3221−3233. (b) Knappke, C. E. I.; Grupe, S.; Gärtner, D.; Corpet, M.; Gosmini, C.; Jacobi von Wangelin, A. Reductive Cross-Coupling Reactions between Two Electrophiles. *Chem. − Eur. J.* **2014**, *20*, 6828−6842. (c) Pellissier, H. Recent developments in enantioselective cobalt-catalyzed transformations. *Coord. Chem. Rev.* **2018**, *360*, 122−168. (d) Dorval, C.; Gosmini, C., Low-valent Cobalt Complexes in C−X Coupling and Related Reactions. In *Cobalt Catalysis in Organic Synthesis*, 2020; pp 163−205.

(2) (a) Ma, W.-Y.; Han, G.-Y.; Kang, S.; Pang, X.; Liu, X.-Y.; Shu, X.-Z. Cobalt-Catalyzed Enantiospecific Dynamic Kinetic Cross-Electrophile Vinylation of Allylic Alcohols with Vinyl Triflates. *J. Am. Chem. Soc.* **2021**, *143*, 15930−15935. (b) Zhang, X.; Wang, J.; Yang, S.-D. Enantioselective Cobalt-Catalyzed Reductive Cross-Coupling for the Synthesis of Axially Chiral Phosphine−Olefin Ligands. *ACS Catal.* **2021**, *11*, 14008−14015.

(3) (a) Liu, W.; Tong, X. Pd(0)-Catalyzed Cyclizative Carboboration of n-Iodo-1,6-diene (n = 1 or 2): Access to Structurally Complex Allylboronates and Alkylboronates. *Org. Lett.* **2019**, *21*, 9396−9400. (b) Chen, X.; Zhao, J.; Dong, M.; Yang, N.; Wang, J.; Zhang, Y.; Liu, K.; Tong, X. Pd(0)-Catalyzed Asymmetric Carbohalogenation: H-Bonding-Driven C(sp3)−Halogen Reductive Elimination under Mild Conditions. *J. Am. Chem. Soc.* **2021**, *143*, 1924−1931. (c) Qiao, J.-B.; Zhang, Y.-Q.; Yao, Q.-W.; Zhao, Z.-Z.; Peng, X.; Shu, X.-Z. Enantioselective Reductive Divinylation of Unactivated Alkenes by Nickel-Catalyzed Cyclization Coupling Reaction. *J. Am. Chem. Soc.* **2021**, *143*, 12961−12967. (d) Chi, X.; Xia, T.; Yang, Y.; Cao, T.; Zhang, D.; Liu, H. Highly diastereoselective synthesis of an octahydro-1H-cyclpenta[c]pyridine skeleton via a Pd/Au-relay catalyzed reaction of (Z)-1-iodo-1,6-diene and alkyne. *Org. Chem. Front.* **2022**, *9*, 3186−3191. (e) Dong, M.; Qi, L.; Qian, J.; Yu, S.; Tong, X. Pd(0)-Catalyzed Asymmetric 7-Endo Hydroacyloxylative Cyclization of 1,6-Enyne Enabled by an Anion Ligand-Directed Strategy. *J. Am. Chem. Soc.* **2023**, *145*, 1973−1981. (f) Ma, Z.; Sun, L.; Zhou, J. S. Catalytic Enantioselective Domino Alkenylation-Alkynylation of Alkenes: Stereoselective Syntheses of 5-7 Membered Azacycles and Carbocycles. *Sci. China: Chem.* **2023**, 1701. (g) Ma, Z.; Sun, L.; Zhou, J. S. Catalytic Enantioselective Alkenylation-Heteroarylation of Olefins: Stereoselective Syntheses of 5-7 Membered Azacycles and Oxacycles. *Chem. Sci.* **2023**, *14*, 3010−3017. (h) Qi, L.; Dong, M.; Qian, J.; Yu, S.; Tong, X. Pd^0-Catalyzed Asymmetric Carbonitratation Reaction Featuring an H-Bonding-Driven Alkyl−Pd^{II}−ONO_2 Reductive Elimination. *Angew. Chem., Int. Ed.* **2023**, *62*, No. e202215397.

(4) (a) Aldeghi, M.; Malhotra, S.; Selwood, D. L.; Chan, A. W. E. Two- and Three-dimensional Rings in Drugs. *Chem. Biol. Drug Des.* **2014**, *83*, 450−461. (b) Taylor, R. D.; MacCoss, M.; Lawson, A. D. G. Rings in Drugs. *J. Med. Chem.* **2014**, *57*, 5845−5859. (c) Vitaku, E.; Smith, D. T.; Njardarson, J. T. Analysis of the Structural Diversity, Substitution Patterns, and Frequency of Nitrogen Heterocycles among U.S. FDA Approved Pharmaceuticals. *J. Med. Chem.* **2014**, *57*, 10257−10274. (d) Talele, T. T. Opportunities for Tapping into Three-Dimensional Chemical Space through a Quaternary Carbon. *J. Med. Chem.* **2020**, *63*, 13291−13315. (e) Bhutani, P.; Joshi, G.; Raja, N.; Bachhav, N.; Rajanna, P. K.; Bhutani, H.; Paul, A. T.; Kumar, R. U. S. FDA Approved Drugs from 2015−June 2020: A Perspective. *J. Med. Chem.* **2021**, *64*, 2339−2381.

(5) Zha, G.-F.; Rakesh, K. P.; Manukumar, H. M.; Shantharam, C. S.; Long, S. Pharmaceutical significance of azepane based motifs for drug discovery: A critical review. *Eur. J. Med. Chem.* **2019**, *162*, 465−494.

(6) Tian, Z.-X.; Qiao, J.-B.; Xu, G.-L.; Pang, X.; Qi, L.; Ma, W.-Y.; Zhao, Z.-Z.; Duan, J.; Du, Y.-F.; Su, P.; Liu, X.-Y.; Shu, X.-Z. Highly Enantioselective Cross-Electrophile Aryl-Alkenylation of Unactivated Alkenes. *J. Am. Chem. Soc.* **2019**, *141*, 7637−7643.

(7) (a) Ackerman, L. K. G.; Lovell, M. M.; Weix, D. J. Multimetallic catalysed cross-coupling of aryl bromides with aryl triflates. *Nature* **2015**, *524*, 454−457. (b) Weix, D. J. Methods and Mechanisms for Cross-Electrophile Coupling of Csp2 Halides with Alkyl Electrophiles. *Acc. Chem. Res.* **2015**, *48*, 1767−1775. (c) Hansen, E. C.; Pedro, D. J.; Wotal, A. C.; Gower, N. J.; Nelson, J. D.; Caron, S.; Weix, D. J. New ligands for nickel catalysis from diverse pharmaceutical heterocycle libraries. *Nat. Chem.* **2016**, *8*, 1126−1130. (d) Wang, X.; Dai, Y.; Gong, H. Nickel-Catalyzed Reductive Couplings. *Top. Curr. Chem.* **2016**, *374*, 43. (e) Wang, K.; Ding, Z.; Zhou, Z.; Kong, W. Ni-Catalyzed Enantioselective Reductive Diarylation of Activated Alkenes by Domino Cyclization/Cross-Coupling. *J. Am. Chem. Soc.* **2018**, *140*, 12364−12368. (f) Anthony, D.; Lin, Q.; Baudet, J.; Diao, T. Nickel-Catalyzed Asymmetric Reductive Diarylation of Vinylarenes. *Angew. Chem., Int. Ed.* **2019**, *58*, 3198−3202. (g) Jin, Y.; Wang, C. Nickel-Catalyzed Asymmetric Reductive Arylalkylation of Unactivated Alkenes. *Angew. Chem., Int. Ed.* **2019**, *58*, 6722−6726. (h) Li, Y.; Ding, Z.; Lei, A.; Kong, W. Ni-Catalyzed enantioselective reductive aryl-alkenylation of alkenes: application to the synthesis of (+)-physovenine and (+)-physostigmine. *Org. Chem. Front.* **2019**, *6*, 3305−3309. (i) Ma, T.; Chen, Y.; Li, Y.; Ping, Y.; Kong, W. Nickel-Catalyzed Enantioselective Reductive Aryl Fluoroalkenylation of Alkenes. *ACS Catal.* **2019**, *9*, 9127−9133. (j) Goldfogel, M. J.;

Huang, L.; Weix, D. J. Cross-Electrophile Coupling. In *Nickel Catalysis in Organic Synthesis*, 2020; pp 183−222; (k) Jin, Y.; Yang, H.; Wang, C. Nickel-Catalyzed Asymmetric Reductive Arylbenzylation of Unactivated Alkenes. *Org. Lett.* **2020**, *22*, 2724−2729. (l) Poremba, K. E.; Dibrell, S. E.; Reisman, S. E. Nickel-Catalyzed Enantioselective Reductive Cross-Coupling Reactions. *ACS Catal.* **2020**, *10*, 8237−8246. (m) Qi, X.; Diao, T. Nickel-Catalyzed Dicarbofunctionalization of Alkenes. *ACS Catal.* **2020**, *10*, 8542−8556. (n) Shu, X.-Z.; Pang, X.; Peng, X. Reductive Cross-Coupling of Vinyl Electrophiles. *Synthesis* **2020**, *52*, 3751−3763. (o) Tu, H.-Y.; Wang, F.; Huo, L.; Li, Y.; Zhu, S.; Zhao, X.; Li, H.; Qing, F.-L.; Chu, L. Enantioselective Three-Component Fluoroalkylarylation of Unactivated Olefins through Nickel-Catalyzed Cross-Electrophile Coupling. *J. Am. Chem. Soc.* **2020**, *142*, 9604−9611. (p) Wei, X.; Shu, W.; García-Domínguez, A.; Merino, E.; Nevado, C. Asymmetric Ni-Catalyzed Radical Relayed Reductive Coupling. *J. Am. Chem. Soc.* **2020**, *142*, 13515−13522. (q) Hewitt, K. A.; Lin, P. C.; Raffman, E. T. A.; Jarvo, E. R. C−C Bond Formation Through Cross-Electrophile Coupling Reactions. In *Comprehensive Organometallic Chemistry IV*, Parkin, G.; Meyer, K.; O'hare, D., Eds.; Elsevier: Oxford, 2022; pp 89−119; (r) Jia, X.-G.; Yao, Q.-W.; Shu, X.-Z. Enantioselective Reductive N-Cyclization−Alkylation Reaction of Alkene-Tethered Oxime Esters and Alkyl Iodides by Nickel Catalysis. *J. Am. Chem. Soc.* **2022**, *144*, 13461−13467.

(8) We attempted to developed a nickel catalyst for asymmetric reductive coupling of iododiene **1a** and phenyl iodide. A nickel catalyst of **L15** promoted the reaction to give product **2b** in good yield and >80% ee. The result will be published elsewhere.

(9) (a) Lee, S. J.; Beak, P. Asymmetric Synthesis of 4,5,6- and 3,4,5,6-Substituted Azepanes by a Highly Diastereoselective and Enantioselective Lithiation−Conjugate Addition Sequence. *J. Am. Chem. Soc.* **2006**, *128*, 2178−2179. (b) Zhu, C.-Z.; Feng, J.-J.; Zhang, J. Rhodium(I)-Catalyzed Intermolecular Aza-[4+3] Cycloaddition of Vinyl Aziridines and Dienes: Atom-Economical Synthesis of Enantiomerically Enriched Functionalized Azepines. *Angew. Chem., Int. Ed.* **2017**, *56*, 1351−1355. (c) Wang, G.-W.; Bower, J. F. Modular Access to Azepines by Directed Carbonylative C−C Bond Activation of Aminocyclopropanes. *J. Am. Chem. Soc.* **2018**, *140*, 2743−2747. (d) Zawodny, W.; Montgomery, S. L.; Marshall, J. R.; Finnigan, J. D.; Turner, N. J.; Clayden, J. Chemoenzymatic Synthesis of Substituted Azepanes by Sequential Biocatalytic Reduction and Organolithium-Mediated Rearrangement. *J. Am. Chem. Soc.* **2018**, *140*, 17872−17877. (e) Yang, T.; Guo, X.; Yin, Q.; Zhang, X. Intramolecular asymmetric reductive amination: synthesis of enantioenriched dibenz-[c,e]azepines. *Chem. Sci.* **2019**, *10*, 2473−2477. (f) Mao, Y.; Gao, Y.; Miao, Z. Research Progress on the Asymmetric Cyclization Synthesis of Seven-Membered Rings via Transition Metal Catalysis. *Chin. J. Org. Chem.* **2022**, *42*, 1904−1924.

(10) (a) Ray, J. K.; Paul, S.; Ray, P.; Singha, R.; Rao, D. Y.; Nandi, S.; Anoop, A. Pd-catalyzed intramolecular sequential Heck cyclization and oxidation reactions: a facile pathway for the synthesis of substituted cycloheptenone evaluated using computational studies. *New J. Chem.* **2017**, *41*, 278−284. (b) Hu, H.; Peng, Y.; Yu, T.; Cheng, S.; Luo, S.; Zhu, Q. Palladium-Catalyzed Enantioselective 7-exo-Trig Carbopalladation/Carbonylation: Cascade Reactions To Achieve Atropisomeric Dibenzo[b,d]azepin-6-ones. *Org. Lett.* **2021**, *23*, 3636−3640.

(11) (a) Moncomble, A.; Le Floch, P.; Gosmini, C. Cobalt-Catalyzed Formation of Symmetrical Biaryls and Its Mechanism. *Chem. − Eur. J.* **2009**, *15*, 4770−4774. (b) Moncomble, A.; Floch, P. L.; Lledos, A.; Gosmini, C. Cobalt-Catalyzed Vinylation of Aromatic Halides Using *β*-Halostyrene: Experimental and DFT Studies. *J. Org. Chem.* **2012**, *77*, 5056−5062.

(12) (a) Xu, H.; Bernskoetter, W. H. Mechanistic Considerations for C−C Bond Reductive Coupling at a Cobalt(III) Center. *J. Am. Chem. Soc.* **2011**, *133*, 14956−14959. (b) Foley, B. J.; Palit, C. M.; Timpa, S. D.; Ozerov, O. V. Synthesis of (POCOP)Co(Ph)(X) Pincer Complexes and Observation of Aryl−Aryl Reductive Elimination Involving the Pincer Aryl. *Organometallics* **2018**, *37*, 3803−3812.

(13) (a) Aresta, M.; Rossi, M.; Sacco, A. Tetrahedral complexes of cobalt(I). *Inorg. Chim. Acta* **1969**, *3*, 227−231. (b) Heinze, K.; Huttner, G.; Zsolnai, L.; Schober, P. Complexes of Cobalt(II) Chloride with the Tripodal Trisphosphane triphos: Solution Dynamics, Spin-Crossover, Reactivity, and Redox Activity. *Inorg. Chem.* **1997**, *36*, 5457−5469. (c) Gray, M.; Hines, M. T.; Parsutkar, M. M.; Wahlstrom, A. J.; Brunelli, N. A.; RajanBabu, T. V. Mechanism of Cobalt-Catalyzed Heterodimerization of Acrylates and 1,3-Dienes. A Potential Role of Cationic Cobalt(I) Intermediates. *ACS Catal.* **2020**, *10*, 4337−4348. (d) Wang, L.; Wang, L.; Li, M.; Chong, Q.; Meng, F. Cobalt-Catalyzed Diastereo- and Enantioselective Reductive Allyl Additions to Aldehydes with Allylic Alcohol Derivatives via Allyl Radical Intermediates. *J. Am. Chem. Soc.* **2021**, *143*, 12755−12765.

(14) (a) Everson, D. A.; Jones, B. A.; Weix, D. J. Replacing Conventional Carbon Nucleophiles with Electrophiles: Nickel-Catalyzed Reductive Alkylation of Aryl Bromides and Chlorides. *J. Am. Chem. Soc.* **2012**, *134*, 6146−6159. (b) Charboneau, D. J.; Brudvig, G. W.; Hazari, N.; Lant, H. M. C.; Saydjari, A. K. Development of an Improved System for the Carboxylation of Aryl Halides through Mechanistic Studies. *ACS Catal.* **2019**, *9*, 3228−3241. (c) Lin, Q.; Diao, T. Mechanism of Ni-Catalyzed Reductive 1,2-Dicarbofunctionalization of Alkenes. *J. Am. Chem. Soc.* **2019**, *141*, 17937−17948.

(15) Compound **3k** showed an EC_{50} value of 10 μM against breast cancer cell line T47D. We thank Dr. Zhendong Zhu at Shenzhen Bay Laboratory for the bioassay.

https://doi.org/10.1021/jacs.3c02829
J. Am. Chem. Soc. 2023, 145, 16464−16473